Cortical Contributions to Imagined Power Grip Task: An EEG-Triggered TMS Study

Houmin Wang, Huixian Zheng, Yu Yang, Kenneth N. K. Fong, and Jinyi Long

***Abstract*— Previous studies have demonstrated that motor imagery leads to desynchronization in the alpha rhythm within the contralateral primary motor cortex. However, the underlying electrophysiological mechanisms responsible for this desynchronization during motor imagery remain unclear. To examine this question, we conducted an investigation using EEG in combination with noninvasive transcranial magnetic stimulation (TMS) during index finger abduction (ABD) and power grip imaginations. The TMS was administered employing diverse coil orientations to selectively stimulate corticospinal axons, aiming to target both early and late synaptic inputs to corticospinal neurons. TMS was triggered based on the alpha power levels, categorized in 20th percentile bins, derived from the individual alpha power distribution during the imagined tasks of ABD and power grip. Our analysis revealed negative correlations between alpha power and motor evoked potential (MEP) amplitude, as well as positive correlations with MEP latency across all coil orientations for each imagined task. Furthermore, we conducted functional network analysis in the alpha band to explore network connectivity during imagined index finger abduction and power grip tasks. Our findings indicate that network connections were denser in the fronto-parietal area during imagined ABD compared to power grip conditions. Moreover, the functional network properties demonstrated potential for effectively classifying between these two imagined tasks. These results provide functional evidence supporting the hypothesis that alpha oscillations may play a role in suppressing MEP amplitude and latency during imagined power grip. We propose that imagined ABD and power grip tasks may activate different populations and densities of axons at the cortical level.**

***Index Terms*— Alpha power, motor imagery, transcranial magnetic stimulation (TMS), I-waves, machine learning.**

Manuscript received 5 July 2023; revised 1 September 2023; accepted 14 September 2023. Date of publication 20 September 2023; date of current version 28 September 2023. This work was supported in part by the National Natural Science Foundation of China under Grant 62276115; in part by the Outstanding Youth Project of Guangdong Natural Science Foundation of China under Grant 2021B1515020076; in part by the Guangdong Provincial Key Laboratory of Traditional Chinese Medicine Informatization under Grant 2021B1212040007; in part by the Fundamental Research Funds for Central Universities; and in part by the Science and Technology Planning Project of Guangdong Province, China, under Grant 2023A0505050092. *(Corresponding author: Jinyi Long.)*

This work involved human subjects or animals in its research. Approval of all ethical and experimental procedures and protocols was granted by The First Affiliated Hospital of Jinan University under Application No. KY-2020-036.

Houmin Wang, Huixian Zheng, and Yu Yang are with the College of Information Science and Technology, Jinan University, Guangzhou 510632, China.

Kenneth N. K. Fong is with the Department of Rehabilitation Sciences, The Hong Kong Polytechnic University Kowloon, Hong Kong, SAR.

Jinyi Long is with the College of Information Science and Technology, Jinan University, Guangzhou 510632, China, also with the Guangdong Key Laboratory of Traditional Chinese Medicine Information Technology, Guangzhou 510632, China, and also with the Pazhou Laboratory, Guangzhou 510335, China (e-mail: jinyil@jnu.edu.cn).

Digital Object Identifier 10.1109/TNSRE.2023.3317813

I. Introduction

THE power grip holds immense significance in our daily routines, yet conditions like stroke can lead to its weakening, dramatically reducing patients' overall quality of life. Notably, there's an established connection between diminished power grip post-stroke and higher mortality rates [1]. Motor imagery (MI) can be defined as "mentally simulating actions without actually doing them" [2], offers a remarkable cognitive function of the human brain that has practical implications in stroke rehabilitation. Studies, such as the one by Llanos et al. have revealed reductions in alpha band (8-13 Hz) power during motor imagery tasks, suggesting potential neural suppression mechanisms [3]. This observation aligns with the pulsed inhibition hypothesis, which posits that alpha band oscillations in electroencephalogram (EEG) activity may contribute to neuronal suppression [4], [5]. Building on these findings, Temporiti et al. demonstrated that motor imagery can significantly enhance functional recovery in patients [6]. Furthermore, Shen et al. innovatively combined motor imagery with the central pattern generator, presenting a novel approach with promising results in the rehabilitation of spinal cord injuries [7]. Collectively, this physiological and experimental evidence underscores the necessity of delving into the neuroscience mechanisms underlying imagined power grip for the purpose of effective functional rehabilitation [8].

To date, the extent of cortical involvement in imagined power grip remains uncertain. However, understanding these neural mechanisms holds significance in advancing brain-computer interface (BCI) systems for motor rehabilitation. Nevertheless, understanding its neural mechanisms of brain is also of great significance for improving the BCI system [9]. A BCI has the capability to identify user-initiated modifications in cerebral signals and convert them into commands for neuroprostheses or robotic arms [10]. Ofner et al. carried out research to discriminate hand movements with respect to the palmar grasp and hand open, and the results achieved a classification accuracy of 68.4% [11]. Movement-related cortical potentials (MRCPs) shape

BCI design [11], [12]. Iturrate et al. differentiated power and precision grips within EEG signals [14]. Enhanced alpha oscillations possibly indicate more top-down control, reflecting finer motor precision [13]. Tao et al. effectively utilized electrophysiological source imaging (ESI) alongside a hybrid feature convolutional neural network (CNN) to effectively address the binary classification challenge of MI-EEG [9]. Iturrate et al.'s multidimensional decoding algorithm achieved grasp type accuracy 70% [13], relevant for post-stroke rehabilitation via BCI [9], [14]. Primate studies reveal corticospinal neuron activity during precision grips [15]. Corticospinal neurons in the primary motor cortex (M1) show task-specific engagement for power and precision grips [15], [16]. Fronto-parietal feedback loops display enhanced interactions in precision grips due to heightened motor control demands [13]. Corticocortical influences on imagined power grip, however, remain unclear.

EEG-based functional connectivity analysis demonstrates brain attributes [17], [18], [19]. Different motor imagery tasks exhibit distinct EEG network patterns [17], [20]. Furthermore, transcranial magnetic stimulation (TMS) can serve as an effective method to explore cortical contributions in the human brain, the existing research has demonstrated that hand-targeted single-pulse TMS can induce diverse descending volleys of current flow [13]. TMS coil orientation affects corticospinal activity [21]. Moreover, PA and AP TMS coil orientations may activate early and late I-waves, respectively, in primates [22]. Imagined power grip engages later synaptic inputs [8]. BCI-triggered TMS demonstrates potential recruitment of these inputs during power grip [8].

Motivated by the above discussions, we hypothesize that there may be a correlation between imagined power grip and index finger abduction (ABD) on alpha power. We also analyzed EEG network connectivity properties on the alpha band. After obtaining significant results in network properties, we effectively used the functional network properties as features. We employed SVM, LDA and KNN classifiers to exploit the differences to classify imagined ABD and power grip, and the highest accuracy of 76.3% was obtained on our dataset. We also proposed employing an alpha power-based TMS BCI system that is triggered at the same time as each 20%-percentile bin from the targeting of individual alpha power distribution was carried out in a pseudorandomized sequence. Subsequently, to verify the corticocortical contributions to the brain power at alpha rhythm in motor imagery hand movements, we employed three distinct TMS coil orientations: latero-medial (LM), posterior-anterior (PA), and anterior-posterior (AP).

This study's key contributions encompass an inverse alpha power-MEP amplitude relationship and denser brain network connections during imagined ABD. These findings support precision grip's demand for heightened interactions. Functional network properties enable accurate motor imagery task classification. Imagined ABD and power grip activate cortical axons differently. Section II presents a detailed description of our methods. Subsequently, in Section III, we present the experimental results obtained. Finally, Section V summarizes the conclusions derived from our current study.

II. Methods

A. Subjects

Thirteen healthy volunteers, all right-handed (8 men, aged 23.4 $\pm$ 2.7 years), were recruited as participants for this study. Prior to the experimental procedures, all participants granted their informed consent prior to their involvement in the study, and the study protocol received ethical approval from the ethics committee at Jinan University. In accordance with the principles stated in the Declaration of Helsinki, the study protocol was implemented. All the subjects reported that they were right-handed, without mental or other illnesses. No subject reported being incapable of concentrating on executing motor imagery tasks. In addition, We assure all subjects that their data will not be used for the general demographic, such as age and sex. All participants actively engaged in the complete duration of the experiment.

B. Experimental Setup

The experiments took place in a quiet laboratory setting. Subjects sat in a comfortable reclining armchair facing a computer monitor placed 1.2 meters in front of them at eye level. Subjects were instructed to sit in a stable and place their hands, resting on the armrests, palm side down. The entire experimental procedure was carried out on a single day, employing consistent EEG and electromyographic (EMG) electrode configurations. Generally, the experiment required 2-2.5 hours to complete all procedures in the present experiment. The experimental flow is shown in Fig. 1A. In each trial of the experiment, subjects were required to relax when a fixation cross was shown for 3-5 s. After the appearance of the fixation cross, a black circle was displayed for 1 s. During this period, the subjects were instructed to make preparations for the motor imagery tasks. Then, the motor imagery task cue image was shown for 5 s. Two distinct types of motor imagery tasks were included, involving either the index finger abduction or the power grip. The cue image appeared randomly. Upon the appearance of the motor imagery cue image on the screen, participants were instructed to engage in sustained mental imagery of the imagined grasping behaviors using their right hand. Fig. 1B indicates the representative alpha oscillations elicited in motor imagery tasks. Note that a decrease in power in alpha rhythm can be observed after the motor imagery tasks (Fig. 1B). The online EEG processing diagram within the BCI system (Fig. 1C). Fig. 2 illustrates a schematic overview of the power calculation diagram implemented in real-time. The online power calculator converted the EEG signal into percentile bins (1-20%, ..., 81-100%) representing the threshold alpha power. Once the power reached the threshold, single-pulse transcranial magnetic stimulation (TMS) was administered to the primary motor cortex (M1) region. The resulting motor evoked potentials (MEPs) were captured from the first dorsal interosseous (FDI) muscle.

C. EMG Recordings

Surface electromyography (EMG) was captured from the first dorsal interosseous (FDI) muscles using a set of bipolar Ag/AgCl electrodes (10-mm diameter). The cathode electrodes

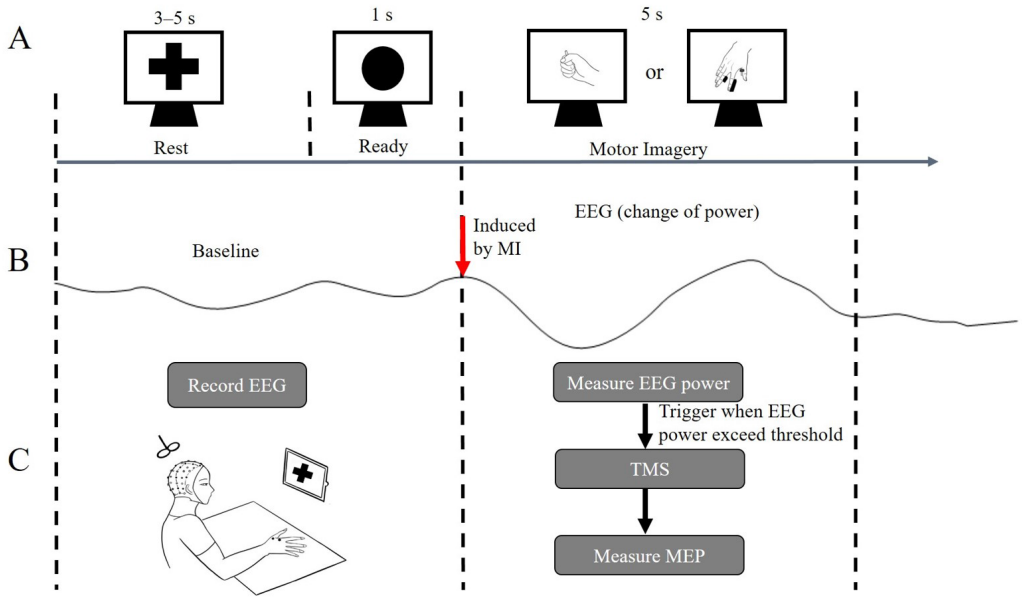

Fig. 1. (A) Experimental paradigm. (B) Representative alpha oscillations elicited in motor imagery tasks. (C) EEG real-time processing flowchart in the real-time BCI system. EEG electrodes are positioned in the vicinity of the right-hand sensorimotor area. EEG signals are calculated by the power online calculator.

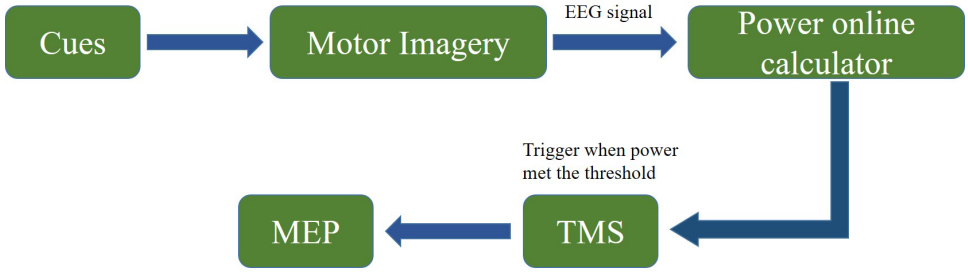

Fig. 2. The EEG online calculation diagram in the present BCI online system. EEG signals are calculated by the power online computational platform. The calculated data was transferred to an analog-to-digital (A/D) converter (CED Micro 1401, Cambridge Electronic Design, UK). When the power met the threshold (20%-power bin), a single-pulse transcranial magnetic stimulation (TMS) is delivered to the M1 area. The MEP is obtained from the FDI muscle.

were positioned directly on the muscle belly, while the anode electrodes were positioned 20 mm distally from the cathode electrodes. The EMG signals were amplified and filtered using a bioamplifier (Neurolog System, Digitimer, UK) with a frequency range of 5-2000 Hz. The signals were then recorded and stored at a sampling rate of 5 kHz using an A/D converter (CED Micro 1401, Cambridge Electronic Design, UK) connected to a computer. The captured data were later analyzed offline utilizing EMG acquisition software (Spike 2). EMG activities exceeding $\pm$ 0.025 mV will be discarded [23]. MEP latency was determined for each trial in every subject and condition. The initiation of the motor evoked potential (MEP) was determined by detecting the point at which the rectified EMG signals exceeded 2 standard deviations (SD) above the average background EMG level. The background EMG level was calculated by measuring the EMG activity 100 ms prior to the stimulus artifact [13].

D. Transcranial Magnetic Stimulation

A TMS stimulator with a figure-8 coil configuration (Magstim BiStim2, UK) was employed, which generated a single-phase current waveform delivered through a 70-mm figure-eight coil. The coil positioning was determined to elicit the maximum MEPs in the target muscle and indicated on the scalp with ink to guarantee precise repositioning of the coil during the entire experiment. The TMS coil was positioned to elicit currents within the brain using three orientations: latero-medial (LM), posterior-anterior (PA), and anterior-posterior (AP). This allowed for targeted activation of corticospinal axons directly, as well as the engagement of both early and late synaptic inputs to corticospinal neurons, depending on the specific orientation used. The resting motor threshold (RMT) was determined as the minimum stimulus intensity required to elicit a minimum of 5 out of 10 MEPs with an amplitude exceeding 50 μV. Subsequently, the stimulus intensity was adjusted to 150% of the RMT for the LM coil orientation and 110% of the RMT for both the PA and AP coil orientations [18]. To ensure direct stimulation (D-wave) of corticospinal neurons at the LM coil orientation, a higher stimulus intensity was administered [24]. In order to mitigate the potential interference of TMS on the EEG signal, we took measures to ensure that the coil did not come into direct contact with the EEG scalp throughout the entire experiment. This was done to minimize any potential artifacts caused by the coil and maintain the integrity of the EEG signal. However, TMS stimulation has an extremely brief duration

(< 10 ms) [8]. In Fig. 1A, a minimum inter-stimulus interval of 9 seconds was implemented, allowing for the trimming of the TMS artifact between each stimulus. The average number of missing trials is 8 ± 3 for the whole.

E. EEG Measurement and Analyses

An online BCI system was developed to enable real-time measurement of alpha power, providing continuous feedback during each trial. EEG signals were captured using a set of five Ag/AgCl electrodes with a diameter of 10 mm. These electrodes were strategically positioned to encompass the sensorimotor hand region, including C3 and additional locations positioned 30 mm anterior, posterior, medial, and lateral to C3. The ground electrode was placed on the forehead, and reference electrodes were placed on both earlobes. The impedance of all channels was carefully monitored and kept below 5 kΩ throughout the entire duration of the experiment. The EEG signals were filtered using a 4th order Butterworth band-pass filter with a frequency range of 0.1 to 100 Hz, and a notch filter at 50 Hz was applied to remove power line interference. The 8-13 frequency band is known as the majority of the motor imagery tasks response range [3]. Therefore, we chose this frequency band for power calculations. Subsequently, the digitized EEG signals were recorded at a sampling rate of 512 Hz using a Neuroscan Synamps2 amplifier. We employed the Informax ICA algorithm by the EEGlab toolbox during the preprocessing stage [25]. The EEG data was streamed to the MATLAB 2014a workspace (The Mathworks, Natick, MA) for real-time analysis. The EEG signal recorded from C3 electrode was subsequently re-referenced using the signals from the four neighboring electrodes. The EEG data was divided into consecutive windows of 512 data points (equivalent to a duration of 1000 ms) with an overlap of 480 points between each segment. Within each segment, the power spectrum density was estimated by applying the Fast Fourier Transform with a Hanning window. To ensure sufficient signal-to-noise ratio for real-time power modulation, the frequency bin containing the average alpha frequency value was extracted from the 3-minute EEG during the resting state recorded while keeping the eyes open before each session. In each block, 125 trials were conducted per condition, targeting twenty percentile bins (1-20%, ..., 81-100%) from the distribution of individual alpha power. The trials were presented in a pseudorandomized order with each trial repeated 25 times. TMS was triggered when the current alpha power value reached the targeted percentile bin in the current trial. This was determined by evaluating the alpha power value and comparing its percentile to the assigned target percentile bin.

F. Brain Functional Network Analysis

To examine the functional network in the brain during imagined index finger abduction and power grip, EEG signals were continuously recorded from 64 scalp electrodes made of Ag/Ag-Cl at a frequency sampling of 1 kHz. Throughout the experiments, the electrical resistance of all electrodes was consistently kept under 5 kΩ, ensuring optimal electrode performance. The positioning of the electrodes followed the extended 10-20 system. A bandpass filter was applied to the EEG signals, with a range of 0.5-100 Hz. Additionally, a 50-Hz notch filter was utilized to eliminate any powerline interference. EEG signals are amplified by the Neuroscan Synamps2 amplifier. The marks generated by the presentation software (E-Prime 3.0) were seamlessly transferred to Curry 8 for further analysis and processing. Preprocessing steps were conducted to remove artifacts and eliminate irrelevant data from the analysis [13]. Epochs of 5,500 ms duration were extracted from the raw EEG data, encompassing a time duration of 500 milliseconds before the onset of stimuli and the entire 5,000 ms duration of the motor imagery task. We removed the global artifacts by average re-referencing. After preprocessing, we constructed the brain network analysis for each data segment. To examine the network properties, functional connectivity was assessed by utilizing coherence as a measure [26]. The fast Fourier transform (FFT) algorithm was employed to calculate the coherence between each trial from a pair of electrodes. Estimating the linear relationship of each pair of electrodes at a specific frequency. Amplitude and phase changes are effective in coherence, and the value ranges from 0 to 1. Two electrodes that work closely have a high coherence value. The coherence is calculated as follows:

$$Coh_{XY}(f) = \frac{\left|\sum_{k=1}^{N} \bar{D}_k(XY)\right|^2}{\sum_{k=1}^{N} \bar{D}_k(XX) \sum_{k=1}^{N} \bar{D}_k(YY)}$$

where $\bar{D}_k(XY) = X_k^{\sharp}(f)Y_k(f)$; $\bar{D}_k(XX) = X_k^{\sharp}(f)X_k(f)$; $\bar{D}_k(YY) = Y_k^{\sharp}(f)Y_k(f)$; N denotes the number of trials; $\sharp$ denotes the complex conjugate.

Based on graph theories, network properties can be used as an effective measurement in functional networks of brains [27]. In the present study, we investigated four fundamental properties of brain networks: clustering coefficient (CC), characteristic path length (CPL), local efficiency (Le), and global efficiency (Ge) [28]. CC and Le provide insights into the local information processing capabilities within the brain network. CPL and Ge are utilized as metrics to assess the efficiency of global information processing within the brain network. These network properties are calculated utilizing the subsequent mathematical expressions:

$$CC = \frac{\sum_{l\in\mathcal{M}} \left(\Phi^{-1} \sum_{j,r\in\mathcal{M}} (\mu_{lj}\mu_{lr}\mu_{jr})^{1/3} \right)}{m}$$

$$Le = \frac{\sum_{l\in\mathcal{M}} \left(\Phi^{-1} \sum_{j,r\in\mathcal{M}, j\neq l} (\mu_{lj}\mu_{lr}[p_{jr}(\mathcal{M}_l)]^{-1})^{1/3} \right)}{m}$$

$$CPL = \frac{\sum_{l\in\mathcal{M}} \left((m-1)^{-1} \sum_{j\in\mathcal{M}, j\neq l} p_{lj} \right)}{m}$$

$$Ge = \frac{\sum_{l\in\mathcal{M}} \left((m-1)^{-1} \sum_{j\in\mathcal{M}, j\neq l} (p_{lj})^{-1} \right)}{m}$$

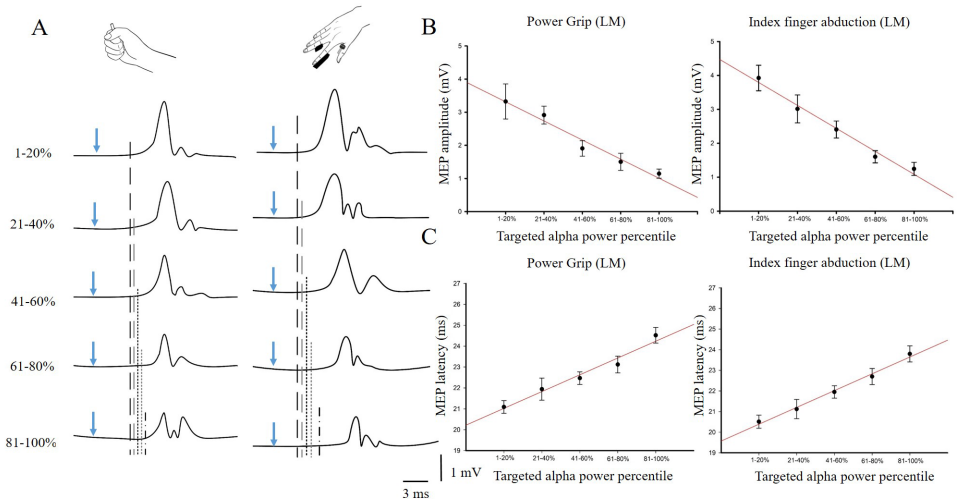

Fig. 3. Effects of alpha rhythm power on corticospinal excitability in LM current. (A) MEPs elicited in the FDI muscle for a representative subject when the TMS coil was oriented in the LM direction during imagined power grip and index finger abduction. Waveforms represent the average of 25 trials. The blue arrow indicates when the stimulus appears. (B) A negative linear relationship between targeted alpha power percentile bin and MEP amplitudes during imagined power grip and imagined index finger abduction. (C) A positive linear relationship between targeted alpha power percentile bin and MEP latencies during imagined power grip and imagined index finger abduction. Error bars indicate SEs. The Pearson correlation results are shown in Table I.

where $\Phi = \sum_{j \in \mathcal{M}} \mu_{lj} \left(\sum_{j \in \mathcal{M}} \mu_{lj} - 1 \right)$; $\mathcal{M}$ denotes the set of electrodes; m denotes the electrode number; p_{lj} denotes the shortest weighted path length between electrode l and electrode j. We analyzed the brain network connectivity with other areas of the whole brain centered on the C3 channel.

G. Imagined Grasping Behavior Classifications Based on BN Features

After the significant results on the brain working mechanism in the two motor imagery tasks were obtained. To investigate the effect of brain network properties on imagined grasping behaviors classification. We employed three machine learning classifiers to distinguish between the two motor imagery tasks (index finger abduction and power grip). The support vector machine classifier model has good classification performance and high training speed [29], [30], [31]. K-nearest neighbor (KNN) and linear discriminant analysis (LDA) are traditional machine learning classifiers [32], and we trained these three classifiers to perform the classification. In the present study, we used network properties as the feature to perform the classification. The raw EEG data underwent preprocessing to eliminate artifacts, as detailed in the "Brain Functional Network Analysis" section, prior to further analysis. Then, we employed the BN properties feature to classify the two imagined grasping behaviors.

H. Data Analysis

The statistical analyses were conducted using IBM SPSS Statistics version 25.0 (IBM, Chicago, IL), and Sigmaplot 11.0 (Systat Software Inc., San Jose, CA, USA) was utilized for data visualization. Data normality and equality of variance were assessed by Shapiro-Wilk's test and Levene's test, respectively, to ensure the appropriateness of the statistical analysis. To assess the assumption of data sphericity, Mauchly's test was employed. When the assumption of sphericity was violated, we utilized the Greenhouse-Geisser correction to adjust the significance of F-values. To examine the differences in each brain network property, a post hoc test (paired t-test) was conducted. To account for multiple comparisons, Pearson correlation analysis was applied. Significance was set at $P < 0.05$. In the text, the group data are reported as the mean $\pm$ standard deviation (SD). MEP responses to the TMS varied across participants. The peak-to-peak MEP amplitude and latency values measured from each MEP were normalized on a per-participant basis to correct for interparticipant differences.

III. Results

A. Correlation Between Alpha Bins and MEPs

Fig. 3 shows the correlations between MEPs (MEP amplitude and latency) and alpha power under the two different motor imagery tasks with the TMS coil positioned in the LM direction. Fig. 3A illustrates the EMG traces recorded from the targeted muscle in a typical individual during different tasks. The regression line fitted to the MEP amplitudes for each individual subject showed a mean negative slope during imagined power grip and ABD (Fig. 3B). The positive relationship with MEP latency in imagined power grip and index finger abduction is shown in Fig. 3C.

After observing a specific impact of alpha power on MEPs of the motor cortex when using the LM-oriented TMS coil. However, additional investigation is needed to better understand the synaptic inputs to corticospinal neurons at both early and late stages. The correlations between MEPs (MEP amplitude and latency) and alpha power under the two different motor imagery tasks with PA and AP currents are shown

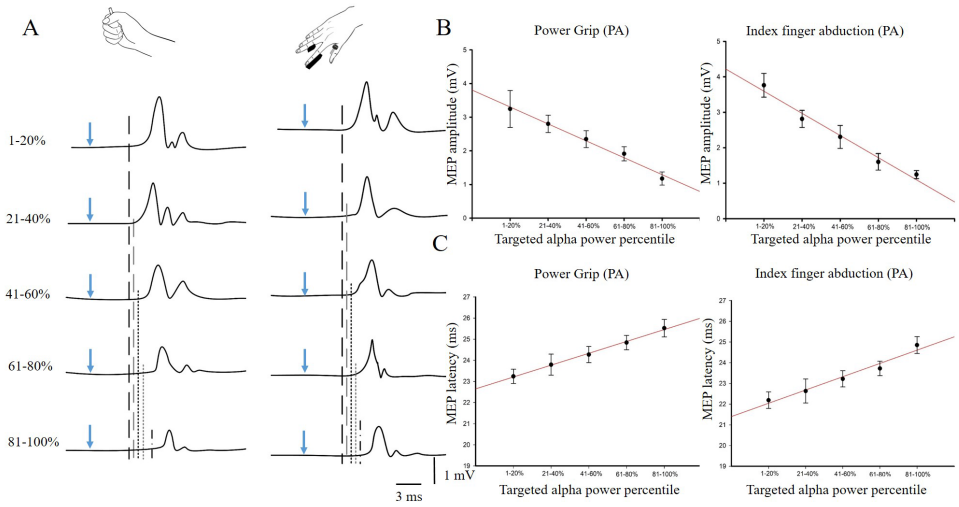

Fig. 4. Effects of alpha rhythm power on corticospinal excitability in PA current. (A) MEPs elicited in the FDI muscle for a representative subject when the TMS coil was oriented in the LM direction during imagined power grip and index finger abduction. Waveforms represent the average of 25 trials. The blue arrow indicates when the stimulus appears. (B) A negative linear relationship between targeted alpha power percentile bin and MEP amplitudes during imagined power grip and imagined index finger abduction. (C) A positive linear relationship between targeted alpha power percentile bin and MEP latencies during imagined power grip and imagined index finger abduction. Error bars indicate SEs. The Pearson correlation results are shown in Table I.

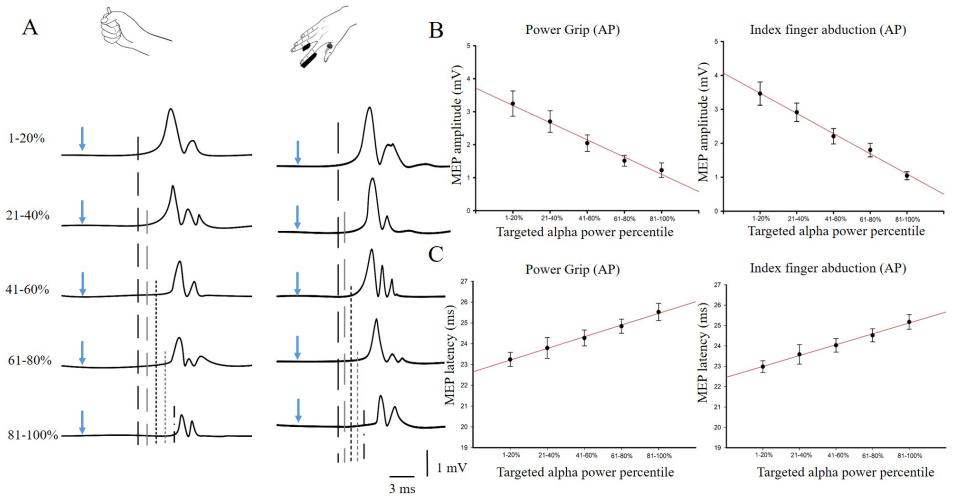

Fig. 5. Effects of alpha rhythm power on corticospinal excitability in AP current. (A) MEPs elicited in the FDI muscle for a representative subject when the TMS coil was oriented in the LM direction during imagined power grip and index finger abduction. Waveforms represent the average of 25 trials. The blue arrow indicates when the stimulus appears. (B) A negative linear relationship between targeted alpha power percentile bin and MEP amplitudes during imagined power grip and imagined index finger abduction. (C) A positive linear relationship between targeted alpha power percentile bin and MEP latencies during imagined power grip and imagined index finger abduction. Error bars indicate SEs. The Pearson correlation results are shown in Table I.

TABLE I
CORRELATION RESULTS IN LM, PA AND AP ORIENTATIONS DURING IMAGINED POWER GRIP AND ABD

		LM	PA	AP
MEP amplitude	Power Grip	R = -0.346, P <0.05	R = -0.604, P <0.05	R = -0.325, P <0.05
	ABD	R = -0.473, P <0.05	R = -0.411, P <0.05	R = -0.481, P <0.05
MEP latency	Power Grip	R = 0.394, P <0.05	R = 0.304, P <0.05	R = 0.661, P <0.05
	ABD	R = 0.526, P <0.05	R = 0.439, P <0.05	R = 0.372, P <0.05

in Fig.4 and Fig.5, respectively. The positive correlation in MEP amplitude and negative correlation in MEP latency in PA and AP orientations. The Pearson correlation results are shown in Table I.

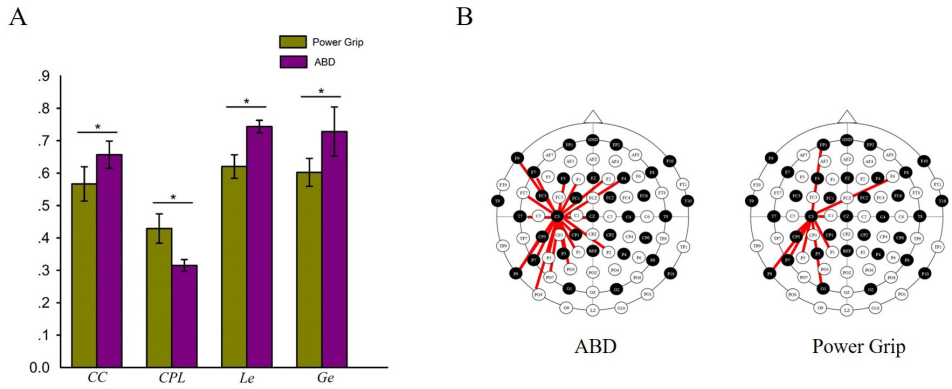

Fig. 6. Brain functional network property results. (A) Average values for the four brain functional network properties in the alpha band under imagined index finger abduction and power grip. The error bars indicate the standard deviations of the average values across all subjects. (B) Network connections with significant differences among the imagined ABD and power grip.

B. Brain Network Properties

Fig.6A displays the mean values of CC, CPL, Le, and Ge for the imagined index finger abduction and power grip tasks in the left hemisphere are presented, considering all participants. A post hoc t-test was conducted, and the results indicated significant differences ($p < 0.05$) between the imagined power grip and imagined index finger abduction tasks in terms of CC, Le, Ge, and CPL. Specifically, imagined power grip exhibited smaller CC, Le, and Ge values ($P < 0.05$) and a higher CPL value ($P < 0.05$) compared to the imagined index finger abduction. This observation suggests that the rates of information interaction within the brain during imagined index finger abduction were higher compared to those during imagined power grip. Fig.6B shows that the network connections exhibiting significant differences ($P < 0.05$) were predominantly distributed in the left fronto-parietal recurrent feedback loops.

C. Classification Results on Our Dataset

In addition to the statistical evaluation, we compared the performance of brain network property features during motor imagery tasks in the current experiment. Brain network connections provide insights into the transmission and processing of information across the brain. In our study, we employed three machine learning classifiers (SVM, LDA, and KNN) and brain network properties in motor imagery classification. We obtained effective classification accuracies in the three classifiers (SVM: $76.3 \pm 3.30\%$; LDA: $59.4 \pm 4.05\%$; KNN: $64.4 \pm 3.12\%$). Our result can be used as a new approach for online machine learning classification. Therefore, the proposed BN property feature has advantages for motor imagery classification.

IV. Discussion

Our findings suggest that the modulation of alpha oscillatory power may inhibit corticospinal neurons exhibiting D-wave and I-wave components during the motor imagery tasks of power grip and index finger abduction. We found that imagined ABD required stronger fronto-parietal recurrent feedback loops, consistent with previous research carried out on grasping behaviors [33]. The brain network property feature was utilized in the three machine learning classifiers for the classification of the two motor imagery tasks, and the classification performance on our datasets demonstrated the highest accuracy of 76.3%.

A. Corticocortical Contributions in Imagined Grasping

Previous research has demonstrated that motor evoked potentials (MEPs) exhibit greater suppression during the power grip task as compared to the index finger abduction task, and this result is explained by the performance of power grip and index finger abduction tasks involves distinct cortical circuits, indicating preferential involvement of different neural networks for each task [33]. The important question in our study is whether different motor imagery tasks influence the corticocortical contributions at the alpha rhythm. Our results show that the correlation with alpha oscillations in the brain is invariant despite different sources of corticospinal excitability undergoes distinct alterations during the imagination of power grip and index finger abduction tasks. Experimental research has demonstrated a modest positive association between mu-alpha power and the amplitude of MEPs in resting conditions by real-time EEG-triggered TMS [3]. The current experiment demonstrates a significant relationship between alpha power and corticospinal excitability. Attenuation exists in alpha power during motor imagery tasks [34]. However, the reason for the significant relationship between alpha power and MEP amplitude is not yet known. Previous research agrees that the results in the first short-interval intracortical facilitation (SICF) peak with the coil directed towards the PA and AP direction indicating the activation of different mechanisms, the PA coil orientation primarily activates early I-waves, while the AP direction predominantly stimulates late I-waves [35], [36]. Thus, our results may be explained by double-pulse TMS stimulation.

Numerous studies have examined the correlation between alpha rhythm power and excitability in the primary somatosensory cortex (S1) as well as the primary motor cortex (M1), and their results are much more complex [37], [38], [39], [40], [41]. Our experiment unable us to obtain definitive findings related to the neuronal rmechanisms responsible for the observed positive association in M1 during imagined

grasping tasks. Notably, our EEG data were collected from the left M1 area, the postcentral gyrus (S1) exhibits greater sensitivity compared to the anterior bank of the central sulcus (M1) area [42], [43]. Because S1 and M1 are interconnected [44], one possible illustration for our result is the relationship between a phase-dependent facilitation of M1 and S1 [45], [46]. Nevertheless, our experiment does not consider the different activation of brain regions in various imagined grasp conditions. This limitation should be solved in further research.

B. Synaptic Activation at Alpha Power

In order to explore the physiological correlates of alpha activity, many combined EEG/MEG and fMRI experiments have been performed [47]. An antagonistic relationship has been suggested between the alpha rhythm and blood oxygen level-dependent (BOLD) signals as indicators of neural activation. Recent investigations have shown a negative correlation in the context of both spontaneous resting state and motor imagery tasks [48]. Given that modulations in MEP amplitude and BOLD activation reflect synaptic activation, a plausible hypothesis arises suggesting a direct relationship between MEP amplitude modulation and BOLD signal alterations. Support for the hypothesis comes from Elena et al. who conducted combined TMS-fMRI studies and observed correlations between TMS effects on behavior and hemodynamic signals in functionally related brain areas [49]. Our findings provide evidence for the correlation between MEP amplitude changes and brain stimulation and the alpha rhythm induced by motor imagery, emphasizing the crucial role of corticocortical contributions in this process. In the current research, we did not test the correlation between synaptic activation and BOLD signals. We cannot exclude the relationship between synaptic activation and BOLD signals. Although we are confident that this limitation did not significantly affect the main findings of our study, future research could investigate the association between synaptic activation and BOLD signal specifically in the context of alpha power.

C. Functional Consideration

Existing research has consistently established a correlation between alpha power and corticospinal excitability in previous studies [29]. In motor imagery experiments, previous studies have reported inconsistent findings regarding the association between alpha power and corticospinal excitability, specifically motor evoked potential (MEP) amplitudes [3] or discovered a negative correlation when employing near-threshold stimulation and subsequent trial categorization methods in limited sample sizes ($N = 4$ [50]; $N = 6$ [51]). Previous results appear at first sight to be no significant results in the M1 area at alpha power. However, the neuronal mechanisms underlying imagined grasping behaviors are more complex, and our data provide different linear relationships in the two motor imagination tasks.

Research findings have indicated that specific corticomotoneuronal cells exhibit higher activity levels during precision grips, whereas others demonstrate increased activity during power grips, despite both types of cells facilitating the same target muscles [52]. Crucially, in humans, the responses associated with the primary motor cortex (M1) exhibited varying differences observed between precision and power grip tasks [33]. In this study, there existed a different relationship between alpha power and MEPs (MEP latency and MEP amplitude) during the two imagined grasping tasks in LM orientation, but there was no significant result in AP and PA orientation. We interpret these findings as an alteration of corticospinal output in the motor system of the primary motor cortex (M1), reflecting state-dependent response changes, which dissociate cortical activity from different imagined grasping behaviors. This finding aligns with the notion of recurrent feedback loops between the frontal and parietal lobes, where relationships are more prominent involving precision grips, given the greater motor behavior demands associated with this specific grasping type. The extent of the primary motor cortex (M1) is more limited compared to the fronto-parietal area. This finding supports the presence of fronto-parietal recurrent feedback loops, which exhibit more pronounced interactions during precision grips, highlighting the greater motor control demands associated with this specific grasping type. However, to acquire mechanistic insights into principles of motor control during motor execution as well, further methodological issues would need to be addressed in future studies.

D. Limitations and Future Work

In the power-triggered BCI system utilized in this study, a consistent set of EEG channels was employed across all subjects. It should be noted that prior research has emphasized the importance of individualized channel selection to mitigate redundant channel information [40], [41]. Previous studies have reported that different EEG signals can be observed in slow-wave time windows (P2 and P3) [53], [54]. In the future, we would like to construct more precise time window brian networks [55]. A study has provided evidence indicating that the optimal selection of EEG channels for recording power may vary inter-subjects due to individual differences in cranial morphology [40]. Therefore, it is beneficial to ascertain the specific channels for each subject in order to acquire the most accurate EEG signal recording. Nevertheless, we applied twenty percentile bins (1-20%, ... , 81-100%) from the distribution of individual alpha power within each block. We cannot exclude other percentile influences in this study. Future work should focus on the distribution of power percentiles.

In the present study, our aim is to make a significant societal impact. In recent advancements, BCI systems have been increasingly utilized in the rehabilitation of individuals with poststroke hemiparesis. Building upon these developments, we aspire to extend the application of our system to enhance the rehabilitation process for stroke patients.

V. Conclusion

In this study, our objective was to explore the cortical contributions in grasping imaginations through the implementation of a power-based motor imagery-triggered BCI system.

Our results reveal that alpha oscillatory power may suppress corticospinal neurons during imagined power grip and imagined ABD. We also confirmed that stronger fronto-parietal recurrent loops are needed in imagined precision grip. Our data provide strong experimental evidence regarding the neuronal mechanisms underlying the cortical communication dynamics in imagined grasping behaviors. We also proposed an effective feature to classify these two MI tasks. In conclusion, our study sheds light on the electrophysiological mechanisms underlying motor imagery by investigating the correlation between alpha power, MEP amplitude, and latency. Furthermore, we unveil unique network connectivity patterns and put forth distinctive activation profiles for the tasks of imagined ABD and power grip. These significant findings enhance our comprehension of the underlying neural mechanisms implicated in motor imagery.

REFERENCES

[1] D. P. Leong et al., "Prognostic value of grip strength: Findings from the prospective urban rural epidemiology (PURE) study," *Lancet*, vol. 386, no. 9990, pp. 266–273, Jul. 2015.

[2] J. Decety, "The neurophysiological basis of motor imagery," *Behavioural Brain Res.*, vol. 77, nos. 1–2, pp. 45–52, May 1996.

[3] C. Llanos, M. Rodriguez, C. Rodriguez-Sabate, I. Morales, and M. Sabate, "Mu-rhythm changes during the planning of motor and motor imagery actions," *Neuropsycholog.*, vol. 51, no. 6, pp. 1019–1026, May 2013.

[4] O. Jensen and A. Mazaheri, "Shaping functional architecture by oscillatory alpha activity: Gating by inhibition," *Frontiers Hum. Neurosci.*, vol. 4, Nov. 2010.

[5] X. Zhang, Y. Guo, B. Gao, and J. Long, "Alpha frequency intervention by electrical stimulation to improve performance in mu-based BCI," *IEEE Trans. Neural Syst. Rehabil. Eng.*, vol. 28, no. 6, pp. 1262–1270, Jun. 2020.

[6] F. Temporiti et al., "Action observation and motor imagery administered the day before surgery enhance functional recovery in patients after total hip arthroplasty: A randomized controlled trial," *Clin. Rehabil.*, vol. 36, no. 12, pp. 1613–1622, Dec. 2022.

[7] X. Shen, X. Wang, S. Lu, Z. Li, W. Shao, and Y. Wu, "Research on the real-time control system of lower-limb gait movement based on motor imagery and central pattern generator," *Biomed. Signal Process. Control*, vol. 71, Jan. 2022, Art. no. 102803.

[8] H. Wang, H. Zheng, H. Wu, and J. Long, "Behavior-dependent corticocortical contributions to imagined grasping: A BCI-triggered TMS study," *IEEE Trans. Neural Syst. Rehabil. Eng.*, vol. 31, pp. 519–529, 2023.

[9] K. Kilteni, B. J. Andersson, C. Houborg, and H. H. Ehrsson, "Motor imagery involves predicting the sensory consequences of the imagined movement," *Nature Commun.*, vol. 9, no. 1, p. 1617, Apr. 2018.

[10] D. M. Taylor, S. I. H. Tillery, and A. B. Schwartz, "Direct cortical control of 3D neuroprosthetic devices," *Science*, vol. 296, no. 5574, pp. 1829–1832, Jun. 2002.

[11] P. Ofner, A. Schwarz, J. Pereira, D. Wyss, R. Wildburger, and G. R. Müller-Putz, "Attempted arm and hand movements can be decoded from low-frequency EEG from persons with spinal cord injury," *Sci. Rep.*, vol. 9, no. 1, pp. 1–15, May 2019.

[12] H. Shibasaki and M. Hallett, "What is the bereitschaftspotential?" *Clin. Neurophysiol.*, vol. 117, no. 11, pp. 2341–2356, Nov. 2006.

[13] I. Iturrate et al., "Human EEG reveals distinct neural correlates of power and precision grasping types," *NeuroImage*, vol. 181, pp. 635–644, Nov. 2018.

[14] X. Zhang et al., "Dynamic corticomuscular multi-regional modulations during finger movement revealed by time-varying network analysis," *J. Neural Eng.*, vol. 19, no. 3, Jun. 2022, Art. no. 036014.

[15] A. Monster, "Corticospinal neurons with a special role in precision grip," *J. Neurophysiol.*, vol. 40, pp. 1432–1443, 1977.

[16] P. Federico and M. A. Perez, "Distinct corticocortical contributions to human precision and power grip," *Cerebral Cortex*, vol. 27, no. 11, pp. 5070–5082, Nov. 2017.

[17] L. Gu, Z. Yu, T. Ma, H. Wang, Z. Li, and H. Fan, "EEG-based classification of lower limb motor imagery with brain network analysis," *Neuroscience*, vol. 436, pp. 93–109, Jun. 2020.

[18] J. Long, L. Shen, Q. Cai, S. Xiao, and Z. Chen, "Novel approach to transfer of coordination skills to the paretic hand by improving the efficiency of cortical network," *IEEE Trans. Neural Syst. Rehabil. Eng.*, vol. 31, pp. 326–334, 2023.

[19] C. Yi et al., "A novel method for constructing EEG large-scale cortical dynamical functional network connectivity (dFNC): WTCS," *IEEE Trans. Cybern.*, vol. 52, no. 12, pp. 12869–12881, Dec. 2022.

[20] A. Athanasiou, M. A. Klados, C. Styliadis, N. Foroglou, K. Polyzoidis, and P. D. Bamidis, "Investigating the role of alpha and beta rhythms in functional motor networks," *Neuroscience*, vol. 378, pp. 54–70, May 2018.

[21] A. K. Datta, L. M. Harrison, and J. A. Stephens, "Task-dependent changes in the size of response to magnetic brain stimulation in human first dorsal interosseous muscle," *J. Physiol.*, vol. 418, no. 1, pp. 13–23, Nov. 1989.

[22] V. Di Lazzaro and U. Ziemann, "The contribution of transcranial magnetic stimulation in the functional evaluation of microcircuits in human motor cortex," *Frontiers Neural Circuits*, vol. 7, p. 18, Feb. 2013.

[23] M. Takemi, T. Maeda, Y. Masakado, H. R. Siebner, and J. Ushiba, "Muscle-selective disinhibition of corticomotor representations using a motor imagery-based brain-computer interface," *NeuroImage*, vol. 183, pp. 597–605, Dec. 2018.

[24] K. J. Werhahn et al., "The effect of magnetic coil orientation on the latency of surface EMG and single motor unit responses in the first dorsal interosseous muscle," *Electroencephalogr. Clin. Neurophysiol./Evoked Potentials Sect.*, vol. 93, no. 2, pp. 138–146, Apr. 1994.

[25] A. Delorme and S. Makeig, "EEGLAB: An open source toolbox for analysis of single-trial EEG dynamics including independent component analysis," *J. Neurosci. Methods*, vol. 134, no. 1, pp. 9–21, Mar. 2004.

[26] P. Fries, "Rhythms for cognition: Communication through coherence," *Neuron*, vol. 88, no. 1, pp. 220–235, Oct. 2015.

[27] K. Yang, L. Tong, J. Shu, N. Zhuang, B. Yan, and Y. Zeng, "High gamma band EEG closely related to emotion: Evidence from functional network," *Frontiers Hum. Neurosci.*, vol. 14, p. 89, Mar. 2020.

[28] Y. Si et al., "Different decision-making responses occupy different brain networks for information processing: A study based on EEG and TMS," *Cerebral Cortex*, vol. 29, no. 10, pp. 4119–4129, Sep. 2019.

[29] E. C. W. van Straaten and C. J. Stam, "Structure out of chaos: Functional brain network analysis with EEG, MEG, and functional MRI," *Eur. Neuropsychopharmacol.*, vol. 23, no. 1, pp. 7–18, Jan. 2013.

[30] T. Song, X. Han, and B. Zhang, "Multi-time-scale optimal scheduling in active distribution network with voltage stability constraints," *Energies*, vol. 14, no. 21, p. 7107, Nov. 2021.

[31] W. F. S. Anqing and J. Tingbo, *Characteristic Parameters Fusion of Acoustic Signals of Transformer Based on 2DPCA*, vol. 35. Guangdong Province, China: Guangdong Electric Power, 2017.

[32] D. S. Bassett and E. Bullmore, "Small-world brain networks," *Neuroscientist*, vol. 12, no. 6, pp. 512–523, Dec. 2006.

[33] T. Tazoe and M. A. Perez, "Cortical and reticular contributions to human precision and power grip," *J. Physiol.*, vol. 595, no. 8, pp. 2715–2730, Apr. 2017.

[34] S. Ruggirello, L. Campioni, S. Piermanni, L. Sebastiani, and E. L. Santarcangelo, "Does hypnotic assessment predict the functional equivalence between motor imagery and action?" *Brain Cognition*, vol. 136, Nov. 2019, Art. no. 103598.

[35] V. Deletis, V. Isgum, and V. E. Amassian, "Neurophysiological mechanisms underlying motor evoked potentials in anesthetized humans.: Part 1. recovery time of corticospinal tract direct waves elicited by pairs of transcranial electrical stimuli," *Clin. Neurophysiol.*, vol. 112, no. 3, pp. 438–444, 2001.

[36] R. Hanajima et al., "Mechanisms of intracortical I-wave facilitation elicited with paired-pulse magnetic stimulation in humans," *J. Physiol.*, vol. 538, no. 1, pp. 253–261, Jan. 2002.

[37] V. Romei, V. Brodbeck, C. Michel, A. Amedi, A. Pascual-Leone, and G. Thut, "Spontaneous fluctuations in posterior α-band EEG activity reflect variability in excitability of human visual areas," *Cerebral Cortex*, vol. 18, no. 9, pp. 2010–2018, Sep. 2008.

[38] G. Thut, A. Nietzel, S. A. Brandt, and A. Pascual-Leone, "α-band electroencephalographic activity over occipital cortex indexes visuospatial attention bias and predicts visual target detection," *J. Neurosci.*, vol. 26, no. 37, pp. 9494–9502, Sep. 2006.

[39] H. van Dijk, J.-M. Schoffelen, R. Oostenveld, and O. Jensen, "Prestimulus oscillatory activity in the alpha band predicts visual discrimination ability," *J. Neurosci.*, vol. 28, no. 8, pp. 1816–1823, Feb. 2008.

[40] Y. Zhang and M. Ding, "Detection of a weak somatosensory stimulus: Role of the prestimulus mu rhythm and its top–down modulation," *J. Cognit. Neurosci.*, vol. 22, no. 2, pp. 307–322, Feb. 2010.

[41] S. R. Jones, D. L. Pritchett, M. A. Sikora, S. M. Stufflebeam, M. Hämäläinen, and C. I. Moore, "Quantitative analysis and biophysically realistic neural modeling of the MEG mu rhythm: Rhythmogenesis and modulation of sensory-evoked responses," *J. Neurophysiol.*, vol. 102, no. 6, pp. 3554–3572, Dec. 2009.

[42] R. Salmelin and R. Hari, "Spatiotemporal characteristics of sensorimotor neuromagnetic rhythms related to thumb movement," *Neuroscience*, vol. 60, no. 2, pp. 537–550, May 1994.

[43] P. Ritter, M. Moosmann, and A. Villringer, "Rolandic alpha and beta EEG rhythms' strengths are inversely related to fMRI-BOLD signal in primary somatosensory and motor cortex," *Human Brain Mapping*, vol. 30, no. 4, pp. 1168–1187, Apr. 2009.

[44] B. M. Hooks, "Sensorimotor convergence in circuitry of the motor cortex," *Neuroscientist*, vol. 23, no. 3, pp. 251–263, Jun. 2017.

[45] P. D. Murray and A. Keller, "Somatosensory response properties of excitatory and inhibitory neurons in rat motor cortex," *J. Neurophysiol.*, vol. 106, no. 3, pp. 1355–1362, Sep. 2011.

[46] C. V. Turco, J. El-Sayes, M. J. Savoie, H. J. Fassett, M. B. Locke, and A. J. Nelson, "Short- and long-latency afferent inhibition; uses, mechanisms and influencing factors," *Brain Stimulation*, vol. 11, no. 1, pp. 59–74, Jan. 2018.

[47] H. Laufs et al., "EEG-correlated fMRI of human alpha activity," *NeuroImage*, vol. 19, no. 4, pp. 1463–1476, Aug. 2003.

[48] G. V. Portnova et al., "Correlation of BOLD signal with linear and nonlinear patterns of EEG in resting state EEG-informed fMRI," *Frontiers Hum. Neurosci.*, vol. 11, p. 654, Jan. 2018.

[49] E. A. Allen, B. N. Pasley, T. Duong, and R. D. Freeman, "Transcranial magnetic stimulation elicits coupled neural and hemodynamic consequences," *Science*, vol. 317, no. 5846, pp. 1918–1921, Sep. 2007.

[50] P. Zarkowski, C. J. Shin, T. Dang, J. Russo, and D. Avery, "EEG and the variance of motor evoked potential amplitude," *Clin. EEG Neurosci.*, vol. 37, no. 3, pp. 247–251, Jul. 2006.

[51] P. Sauseng, W. Klimesch, C. Gerloff, and F. C. Hummel, "Spontaneous locally restricted EEG alpha activity determines cortical excitability in the motor cortex," *Neuropsychologia*, vol. 47, no. 1, pp. 284–288, Jan. 2009.

[52] M. A. Maier, K. M. Bennett, M. C. Hepp-Reymond, and R. N. Lemon, "Contribution of the monkey corticomotoneuronal system to the control of force in precision grip," *J. Neurophysiol.*, vol. 69, no. 3, pp. 772–785, Mar. 1993.

[53] R. Ding, P. Li, W. Wang, and W. Luo, "Emotion processing by ERP combined with development and plasticity," *Neural Plasticity*, vol. 2017, pp. 1–15, Jul. 2017.

[54] E. O. Flores-Gutiérrez et al., "Metabolic and electric brain patterns during pleasant and unpleasant emotions induced by music masterpieces," *Int. J. Psychophysiol.*, vol. 65, no. 1, pp. 69–84, 2007.

[55] F. Li et al., "The time-varying networks in p300: A task-evoked EEG study," *IEEE Trans. Neural Syst. Rehabil. Eng.*, vol. 24, no. 7, pp. 725–733, Jul. 2016.